Disproportionation of Nitric Oxide Promoted by a Mn Tropocoronand

Katherine J. Franz and Stephen J. Lippard*

Contribution from the Department of Chemistry, Massachusetts Institute of Technology, Cambridge, Massachusetts 02139

Received April 24, 1998

Abstract: The synthesis and characterization of the divalent tropocoronand, [Mn(THF)(TC-5,5)] (**1**), are described. Compound **1** reacts with NO to afford a discrete mononitrosyl [Mn(NO)(TC-5,5)] (**2**), which was isolated and shown formally to contain the $\{Mn^{III}NO^{-}\}^{2+}$ fragment by infrared spectroscopy, normal coordinate analysis, X-ray crystallography, and SQUID susceptometry. The Mn center in **2** has idealized trigonal bipyramidal geometry with the NO ligand occupying a coordination site in the equatorial plane. The Mn−N−O bond angle is nearly linear, 174.1(3)°. Compounds **1** and **2** react with excess NO to afford N_2O and [Mn(NO_2)(TC-5,5)] (**3**). The X-ray structure of **3** reveals coordination of the nitrito ligand through one oxygen atom, the Mn−O bond length being 2.09(4) Å. The other oxygen atom interacts weakly with the manganese center at a distance of 2.61(5) Å. Quantitation by gas chromatographic analysis of released N_2O confirms that 1 equiv forms for each molecule of **2** which converts to **3**. Infrared spectroscopic experiments with ^{14}NO and ^{15}NO suggest that a dinitrosyl intermediate is present during the reaction, mechanistic aspects of which are discussed.

Introduction

The reactions of nitric oxide with transition metal ions are of fundamental chemical interest as well as being key to a number of biological and environmental processes. NO is essential for mediating intercellular communication, but its oxidation to NO_2, N_2O_3, and $OONO^-$ can lead to cytotoxic DNA- and protein-damaging events in vivo.[1] The interconversions of NO, NO_x, and N_2O have significant environmental consequences, for these molecules are recognized as both ozone-depleting agents and greenhouse gases.[2] One pathway for interconverting these species is the disproportionation of NO, shown in eq 1.[3] Although NO is thermodynamically unstable,[4]

$$3NO \rightarrow N_2O + NO_2 \qquad (1)$$

it is kinetically inert and generally requires a catalyst to undergo this disproportionation reaction.[5,6] An early example of such a catalyst was $[Co(NH_3)_6]^{2+}$, which forms an isolable nitrosyl species but reacts further with excess NO to afford nitrite ion and release nitrous oxide gas.[7] The proposed mechanism, in which a second NO attacks the coordinated nitrosyl to give a hyponitrito intermediate, $[Co(NH_3)_5(N_2O_2)]^{2+}$, was later reinforced by an X-ray crystal structure determination of a dinuclear cobalt complex in which the two cobalt atoms are asymmetrically bridged by hyponitrito ($N_2O_2^{2-}$) ion,[8] as shown below. This product presumably results from the reaction of the Co^{II} starting material with the putative Co^{III} hyponitrito intermediate.[7]

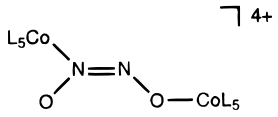

Ethylenediamine (en) complexes of Co^{II} have also displayed an ability to disproportionate NO.[9]

More recently, similar reactivity has been described in attempts to model the copper-containing metalloenzyme nitrite reductase.[10,11] Mononuclear copper nitrosyl compounds were prepared by using sterically protected tris(pyrazolyl)borate (Tp) ligands.[12,13] Less crowded Tp ligands also formed Cu(NO) complexes, but converted to Cu^{II} nitrito species and N_2O when exposed to excess NO, as indicated in Scheme 1.[10,14] Kinetic studies ruled out dimerization of copper species as a rate-limiting step, but could not differentiate between a mononuclear hyponitrite or a dinitrosyl intermediate.[10] The formation of N_2O by these well-defined complexes provides a possible model for copper-mediated N_2O production in biological[15] as well as heterogeneous catalytic systems.[10]

Given the reactivity of both Co and Cu nitrosyl compounds with NO, we were interested in exploring the reactivity of other transition metal centers beyond the formation of discrete NO

(1) Marnett, L. J. *Chem. Res. Toxicol.* **1996**, *9*, 807−808.
(2) Trogler, W. C. *J. Chem. Educ.* **1995**, *72*, 973−976.
(3) Mingos, D. M. P.; Sherman, D. J. *Advances in Inorganic Chemistry*; Academic Press: 1989; Vol. 34, pp 293−377.
(4) Melia, T. P. *J. Inorg. Nucl. Chem.* **1965**, *27*, 95−98.
(5) Bottomley, F. *Reactions of Coordinated Ligands*; Plenum: New York, 1989; Vol. 2, pp 115−222.
(6) Richter-Addo, G. B.; Legzdins, P. *Metal Nitrosyls*; Oxford University: New York, 1992.
(7) Gans, P. *J. Chem. Soc. (A)* **1967**, 943−946.
(8) Hoskins, B. F.; Whillans, F. D.; Dale, D. H.; Hodgkin, D. C. *Chem. Commun.* **1969**, 69−70.
(9) Gwost, D.; Caulton, K. G. *Inorg. Chem.* **1974**, *13*, 414−417.
(10) Ruggiero, C. E.; Carrier, S. M.; Tolman, W. B. *Angew. Chem., Int. Ed. Engl.* **1994**, *33*, 895−897.
(11) Paul, P. P.; Karlin, K. D. *J. Am. Chem. Soc.* **1991**, *113*, 6331−6332.
(12) Carrier, S. M.; Ruggiero, C. E.; Tolman, W. B.; Jameson, G. B. *J. Am. Chem. Soc.* **1992**, *114*, 4407−4408.
(13) Ruggiero, C. E.; Carrier, S. M.; Antholine, W. E.; Whittaker, J. W.; Cramer, C. J.; Tolman, W. B. *J. Am. Chem. Soc.* **1993**, *115*, 11285−11298.
(14) Tolman, W. B. In *Mechanistic Bioinorganic Chemistry*, Thorp, H. H., Pecoraro, V. L., Eds.; Advances in Chemistry 246; American Chemical Society: Washington, DC, 1995; pp 195−217.
(15) Averill, B. A. *Angew. Chem., Int. Ed. Engl.* **1994**, *33*, 2057−2058.

S0002-7863(98)01410-3 CCC: $15.00
Published on Web 08/22/1998

Scheme 1

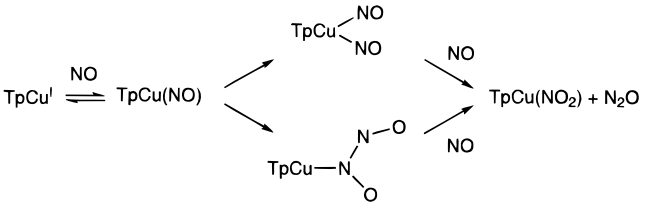

adducts. We were particularly curious about manganese, a ubiquitous biological metal ion that often participates in redox reactions.[16] Although the Mn−NO linkage is well established for mononuclear coordination and organometallic compounds,[17−26] none of these compounds has demonstrated any further reactivity toward NO. Previous work in our laboratory has demonstrated that metal tropocoronand complexes, [M(TC-*n*,*m*)], have properties of structure and reactivity which are distinct from their

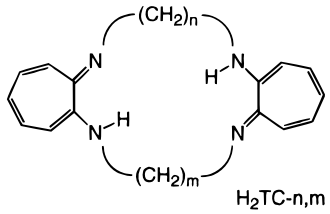

porphyrin or salen counterparts.[27,28] The strongly donating nature of the tropocoronand ligand system, coupled with the ability to access different metal geometries and electrochemical potentials by altering the size of the macrocycle through changes in the number of methylene linker chain atoms, $n + m$, make these tetraazamacrocycles attractive ligands. We have therefore studied the chemistry of Mn tropocoronand complexes, specifically to explore their reactions with NO. Here we describe the synthesis of [Mn(THF)(TC-5,5)], its reactions with NO to form a stable nitrosyl complex, and the first demonstration of Mn-mediated NO disproportionation chemistry to afford N_2O and a well-characterized, novel Mn−ONO complex.

Experimental Section

General Information. All reactions were carried out under nitrogen in a glovebox or by using standard Schlenk techniques. Pentane and THF were freshly distilled from sodium benzophenone ketyl under nitrogen. Dichloromethane and dichloroethane were distilled from CaH_2 under nitrogen. The ligand H_2(TC-5,5) was prepared as described in the literature.[29] [Mn(OTf)$_2$(CH$_3$CN)$_2$] was prepared by a known procedure.[30] Nitric oxide (Matheson, 99%) and ^{15}NO (Aldrich, 99%) were purified from higher nitrogen oxides by passage through a column of NaOH pellets and a mercury bubbler, and kept over mercury in gas storage bulbs. Analysis by GC revealed no other contaminants at the limit of the TC detector, about 30 nM. All other reagents were obtained commercially and not purified further. UV−visible spectra were recorded on a Cary 1 E spectrophotometer, and IR spectra were taken on a Bio Rad FTS-135 instrument with Win-IR software. Solid samples were pressed into KBr pellets; solution samples were prepared in an airtight Graseby-Specac solution cell with CaF_2 or KBr windows, or in a Graseby-Specac variable-temperature cell equipped with CaF_2 windows for measurements at low temperature.

Synthetic Procedures. [Mn(THF)(TC-5,5)] (1). A portion of H_2-(TC-5,5) (173 mg, 0.46 mmol) was dissolved in 10 mL of THF to give a bright yellow solution. *n*-Butyllithium (0.60 mL, 0.96 mmol of 1.6 M solution in hexanes, 2 equiv) was added via syringe. An orange solution resulted, which immediately turned dark green upon addition of [Mn(OTf)$_2$(CH$_3$CN)$_2$] (210 mg, 0.48 mmol, 1 equiv). After the solution was stirred for 4 h, the solvent was removed in vacuo and the green solid was triturated twice with 3 mL of pentane. The powder was extracted into 12 mL of CH_2Cl_2 and filtered through Celite. The solvent was again removed in vacuo and the product was triturated twice with 3 mL of pentane. Dark green rhombic plates (125 mg, 54% yield) suitable for X-ray crystallography were grown from pentane diffusion into a THF solution at −30 °C. FTIR (KBr, cm^{-1}): 2917, 1589(s), 1507(s), 1385, 1352, 1329, 1261(s), 1224(s), 1195, 1044, 983, 937, 888, 864, 751, 710(s), 612, 573, 472. UV−vis (THF, M^{-1} cm^{-1}): 294 (51 000), 386 (36 700), 446 (17 800), 474 nm (18 600). Anal. Calcd for $MnC_{28}H_{38}N_4O$: C, 67.05; H, 7.64; N, 11.17. Found: C, 66.57; H, 7.11; N, 11.67.

[Mn(NO)(TC-5,5)] (2). A portion of **1** (105 mg, 0.21 mmol) was dissolved in 10 mL of THF in a 25 mL, thick-walled, round-bottom flask equipped with a screw-top Teflon stopcock and a sidearm for attachment onto a high-vacuum manifold. This green solution was subjected to 3 freeze−pump−thaw cycles before NO gas (0.25 mmol) was transferred under vacuum to the solution. The complete transfer of NO was facilitated by submerging the reaction flask in a liquid N_2 bath. The color turned deep red immediately upon exposure to NO. The reaction was allowed to stir for 2 h as the solution warmed to room temperature. The solvent was removed in vacuo, and X-ray quality crystals were grown in the drybox by pentane diffusion into a dichloroethane solution at −30 °C (72 mg, 74% yield). FTIR (KBr, cm^{-1}): 1662 (s, ν_{NO}), 1587 (s), 1505 (s), 1430 (s), 1340, 1263 (s), 1229 (s), 1044, 1014, 979 (w), 931 (w), 867 (w), 821 (w), 789 (w), 733 (s), 565 (w), 548 (w), 503 (w), 429 (w). FTIR: 1680 (ν_{NO}, THF); 1676 (ν_{NO}, CH_2Cl_2). UV−vis (THF) nm (M^{-1} cm^{-1}): 276 (31 300), 305 (22 600), 360 (15 800), 424 (20 400), 516 (6 900), 795 (1 100). Magnetic moment by SQUID susceptometry: μ_{eff}, 4.3(1) μ_B, 300 K. Anal. Calcd for $MnC_{24}H_{30}N_5O$: C, 62.74; H, 6.58; N, 15.24. Found: C, 62.45; H, 6.37; N, 14.83.

[Mn(NO$_2$)(TC-5,5)] (3). (a) Method A. A 10-mL CH_2Cl_2 solution of **1** (45 mg, 0.09 mmol) in a 25 mL Schlenk flask was purged with excess NO for 2−3 min. The green solution immediately turned deep red upon exposure to NO. The solvent was evacuated after the reaction had stirred for 2 h under an NO atmosphere. Crystals suitable for X-ray diffraction were grown by pentane diffusion into a THF solution at −30 °C in the drybox (37 mg, 86% yield).

(b) Method B. A 10-mL CH_2Cl_2 solution of **1** (38 mg, 0.076 mmol) was added to a CH_2Cl_2 slurry of $AgNO_2$ (12 mg, 0.08 mmol). The color rapidly changed from green to dark red. The mixture was filtered to remove Ag(s) after the reaction had stirred for 1 h. The solvent was evacuated and the material was recrystallized from pentane diffusion into a THF solution at −30 °C (18 mg, 50% yield). FTIR (KBr cm^{-1}): 1588 (s), 1506 (s), 1413, 1383, 1338, 1265 (s), 1230 (s), 1103, 1041 (s), 974, 937, 886, 868, 641, 549, 484. UV−vis (THF) nm (M^{-1} cm^{-1}): 275 (26 600), 305 (21 400), 356 (11 800), 424

(16) Lippard, S. J.; Berg, J. M. *Principles of Bioinorganic Chemistry*; University Science: Mill Valley, CA, 1994.
(17) Coleman, W. M.; Taylor, L. T. *J. Am. Chem. Soc.* **1978**, *100*, 1705−1710.
(18) Scheidt, W. R.; Hatano, K.; Rupprecht, G. A.; Piciulo, P. L. *Inorg. Chem.* **1979**, *18*, 292−299.
(19) Wayland, B. B.; Olson, L. W.; Siddiqui, Z. U. *J. Am. Chem. Soc.* **1976**, *98*, 94−97.
(20) Cooper, D. J.; Ravenscroft, M. D.; Stotter, D. A.; Trotter, J. *J. Chem. Res.* **1979**, 3359−3384.
(21) Stevens, R. E.; Gladfelter, W. L. *Inorg. Chem.* **1983**, *22*, 2034−2042.
(22) Sheridan, J. B.; Geoffroy, G. L.; Rheingold, A. L. *J. Am. Chem. Soc.* **1987**, *109*, 1584−1586.
(23) Frenz, B. A.; Enemark, J. H.; Ibers, J. A. *Inorg. Chem.* **1969**, *8*, 1288−1293.
(24) Pike, R. D.; Ryan, W. J.; Lennhoff, N. S.; Van Epp, J.; Sweigart, D. A. *J. Am. Chem. Soc.* **1990**, *112*, 4798−4804.
(25) Nietlispach, D.; Bosch, H. W.; Berke, H. *Chem. Ber.* **1994**, *127*, 2403−2415.
(26) Barratt, D. S.; McAuliffe, C. A. *J. Chem. Soc., Dalton Tans.* **1987**, 2497− 2501.
(27) Scott, M. J.; Lippard, S. J. *Inorg. Chim. Acta* **1997**, *263*, 287−299.
(28) Jaynes, B. S.; Ren, T.; Masschelein, A.; Lippard, S. J. *J. Am. Chem. Soc.* **1993**, *115*, 5589−5599.
(29) Davis, W. M.; Roberts, M. M.; Zask, A.; Nakanishi, K.; Nozoe, T.; Lippard, S. J. *J. Am. Chem. Soc.* **1985**, *107*, 3864−3870.
(30) Bryan, P. S.; Dabrowiak, J. C. *Inorg. Chem.* **1975**, *14*, 296−299.

Table 1. Experimental Details for X-ray Diffraction Studies

compound	[Mn(THF)(TC-5,5)] **1**	[Mn(NO)(TC-5,5)] **2**	[Mn(NO_2)(TC-5,5)] **3**
formula	$MnC_{28}H_{38}N_4O$	$MnC_{24}H_{30}N_5O$	$MnC_{24}H_{30}N_5O_2$
formula wt (g mol^{-1})	501.56	459.47	457.47
cryst sys	triclinic	monoclinic	monoclinic
space group	$P\bar{1}$	$P2_1/c$	$C2/c$
a (Å)	10.8822(9)	9.190(4)	16.3396(7)
b (Å)	11.2549(9)	10.182(3)	13.2519(5)
c (Å)	12.377(1)	23.199(7)	10.4791(4)
α (deg)	103.753(10)		
β (deg)	106.881(10)	94.55(2)	92.514(1)
γ (deg)	110.041(10)		
V (Å^3)	1263.3(3)	2164.0(12)	2266.9(2)
Z	2	4	4
ρ_{calcd} (g cm^{-1})	1.319	1.410	1.393
abs coeff (mm^{-1})	0.550	0.637	0.614
temp K	188(2)	188(2)	188(2)
radiation λ (Å)	0.71073	0.71073	0.71073
reflcns collected	3334	12620	6894
data/parameter	3334/308	4919/280	2603/160
R (%)[a]	5.42	6.35	4.67
wR^2 (%)[b]	11.18	10.42	12.34
crystal size (mm)	0.26 × 0.13 × 0.05	0.2 × 0.18 × 0.04	0.08 × 0.34 × 0.56
max/min peak, e/Å^3	0.24/−0.27	0.33/−0.50	0.81/−0.38

[a] $R = \sum||F_o| - |F_c||/\sum|F_o|$. [b] $wR^2 = \{\sum[w(F_o^2 - F_c^2)^2]/\sum[w(F_o^2)^2]\}^{1/2}$.

(21 800), 510 (6 500). Anal. Calcd for $MnC_{24}H_{30}N_5O_2$: C, 60.63; H, 6.36; N, 14.73. Found: C, 60.66; H, 6.77; N, 15.03.

X-ray Crystallography. Single crystals were mounted on quartz fibers with Paratone N (Exxon) and transferred rapidly to the −85 °C cold stream of a Bruker (formerly Siemens) CCD X-ray diffraction system controlled by a pentium-based PC running the SMART software package.[31] The general procedures for data collection and reduction followed those reported elsewhere.[32] Empirical absorption corrections were calculated and applied from the SADABS program.[33] Structures were solved by the direct methods program XS, and refinements were carried out with XL, both part of the SHELXTL program package.[34] Non-hydrogen atoms were refined by a series of least-squares cycles. All hydrogen atoms were assigned idealized positions and given a thermal parameter 1.2 times the thermal parameter of the carbon atom to which each was attached. Experimental details are provided in Table 1.

The NO_2 group in the crystal lattice of compound **3** is disordered over two positions. In space group $C2/c$, a 2-fold axis passing through Mn and the nitrite N atom relates the oxygen atoms by symmetry. As a consequence, the structure could mistakenly be interpreted as one in which the nitrite is bound to the metal center with equivalent Mn−O bond lengths.[35] Severely elongated thermal ellipsoids for the N and O atoms, however, indicated probable disorder of the NO_2 group. To model this disorder, the oxygen atom was assigned two positions, the nitrogen atom was displaced from its special position on the C_2 symmetry axis, and the site occupancies for the disordered position were fixed at one-half. Another nitrogen and two oxygen atoms were thus generated by symmetry. Successful refinement was achieved by constraining the Mn and nitrite atoms to lie in a common plane. The resulting asymmetric structure has been seen in two other crystal forms of the complex which do not have imposed symmetry, further bolstering our confidence in this refinement strategy.[35]

Gas Chromatographic Analyses. Gas chromatography was performed on a Hewlett-Packard 5890 instrument equipped with a thermal conductivity (TC) detector and a 6 ft Haysep packed column. The column flow rate of He carrier gas was 23 mL/min at 35 °C. Under these conditions, the retention times (min) for various gases were determined as N_2 (0.97), NO (1.11), NO_2 (3.6), and N_2O (4.6−4.8). Reactions were performed in 5.0 mL of CH_2Cl_2 in a 10 mL thick-walled flask with a sidearm vacuum adapter, sealed by a Teflon screw top. A gas inlet valve attached to the body of the flask allowed for direct syringe access into the headspace for easy sampling.

In a typical experiment, a solution of **1** (14.6 mg, 0.029 mmol) in 5.0 mL of CH_2Cl_2 was prepared in a drybox and sealed in the reaction flask. The solution was subjected to 3 freeze−pump−thaw cycles on a high vacuum line, and a known quantity of NO (0.146, 5 equiv) was transferred under vacuum. The flask was submerged in liquid N_2 to ensure complete transfer of NO and to condense all volatile gases. The flask was sealed and warmed to room temperature. After the mixture was stirred for 2 days, the pressure was carefully equilibrated to atmospheric with N_2. The headspace was sampled by inserting a needle through the gas-inlet adapter, which was protected from air with a rubber septum; 25-μL aliquots of the headspace were withdrawn with a Hamilton gastight syringe for GC injections. Quantitation of NO and N_2O in the headspace was achieved by comparing the average peak areas from at least three injections to previously prepared standard curves.

Standards were treated in the same manner as the reaction samples to account for the solubility of the gases. The reaction flask was charged with 5.0 mL of CH_2Cl_2 and subjected to 3 freeze−pump−thaw cycles. A known amount of NO was transferred to the flask under vacuum. The headspace was then equilibrated to atmospheric pressure with N_2, and 25 μL of the headspace was injected onto the GC. At least three injections were made for each standard, and the procedure was repeated to generate 5 points on a calibration curve which plotted millimoles of NO added vs GC peak area.

A similar procedure was used to create an N_2O calibration curve. In this case, standard amounts of N_2O were added to the flask via a gastight syringe from a sample of N_2O at known pressure.

Magnetic Susceptibility Measurements. The variable-temperature magnetic susceptibilities of an 18 mg solid sample of **2** and a 13.5 mg sample of **3** were measured by using a Quantum Design MPMS SQUID susceptometer. The samples were loaded in a drybox in gel capsules and suspended in plastic straws. Field dependence studies at 5 and

(31) *SMART. 4.0*; Bruker Analytical X-ray Systems; Madison, WI, 1994.

(32) Feig, A. L.; Bautista, M. T.; Lippard, S. J. *Inorg. Chem.* **1996**, *35*, 6892−6898.

(33) Program written by Professor George Sheldrick at the University of Göttingen that corrects data collected on Bruker CCD and multiwire detectors for absorption and decay.

(34) *SHELXTL:* Structure Analysis Program. 5.1; Bruker Analytical X-ray Systems; Madison, WI, 1997.

(35) In addition to the solution in $C2/c$ reported here, compound **1** has been crystallized and the structure determined in the space groups *Pbca* and $P2_1/n$. X-ray data for crystals grown from $Cl(CH_2)_2Cl/C_5H_{12}$: *Pbca*, a = 12.310(4) Å, b = 18.517(6) Å, c = 19.428(7) Å, V = 4428(3) Å^3, Z = 8, T = 188(2) K, R = 8.12%, wR^2 = 16.83%. X-ray data for crystals grown from THF/C_5H_{12}: $P2_1/n$: a = 16.3227(7) Å, b = 16.8720(6) Å, c = 16.7016(7) Å, β = 102.372(1)°, V = 4492.7(3) Å^3, Z = 8, T = 188(2)°, R = 9.35%, wR^2 = 21.72%. In these latter space groups, the nitrite is not disordered. The metrical parameters of the disordered Mn(NO_2) unit in $C2/c$ are consistent with those of the other solutions.

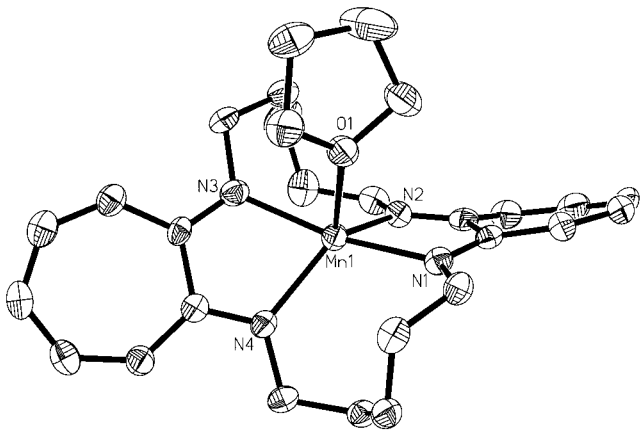

Figure 1. ORTEP diagram of [Mn(THF)(TC-5,5)] **(1)** showing selected atom labels and 50% probability ellipsoids for all non-hydrogen atoms.

150 K showed a linear dependence of magnetization vs field strength from 0 to 10 000 G for both compounds. The data were collected at 5000 G in the temperature range from 5 to 300 K. The infrared spectrum of **2** following the measurement was unchanged, confirming that the sample had not oxidized during the procedures required to obtain the data. The susceptibilities of the straw and gel capsule were measured at the same field and temperatures for accurate correction of their contribution to the total measured susceptibility. A diamagnetic correction of -241×10^{-6} emu·mol^{-1} was calculated from Pascal's constants.[36] The effective magnetic moments (μ_{eff}) were calculated from the following expression, $\mu_{eff} = 2.828(\chi T)^{1/2}$, and found to vary between 4 and 4.3 μ_B in **2**, but remain nearly constant at 5.0 μ_B in **3**, in the range 50−300 K. Below 50 K, the values drop abruptly in both compounds. This behavior is characteristic of zero-field splitting (zfs) effects, so a least-squares routine in Kaleidagraph 3.0 (Abelbeck Software) was employed to fit the χ vs T data to the $S = 2$ zfs expression, derived from the Hamiltonian $H = DS_z^2 + g\mu_B\mathbf{H}\cdot\mathbf{S}$,[37] where D is the zfs parameter.

Vibrational Analyses. Normal-mode analysis was performed on a Silicon Graphics Indigo workstation with the Svib program.[38] Cartesian coordinates for the Mn−N−O fragment were obtained from the X-ray structure of **2** and input to the program to generate a potential energy matrix. Incorporating force constants, the program constructs and solves the vibrational secular equation.[39] The three principal and three interaction force constants associated with the MNO oscillator were refined by least-squares fitting of the experimental frequencies (1662, 527, and 504 cm^{-1} for ^{14}NO and 1628, 523, and 499 cm^{-1} for ^{15}NO). The calculated frequencies corresponded to the experimental frequencies within 0.03 to 0.84% error.

Results and Discussion

Synthesis and Structural Characterization. The manganese tropocoronand complex [Mn(THF)(TC-5,5)] (**1**) was obtained in good yield by reaction of $[Mn(OTf)_2(CH_3CN)_2]$ with the dilithium salt of TC-5,5 in THF. To accommodate internal strain at the methylene linker chains of the TC-5,5 ligand,[40,41] the tropolone rings must twist away from coplanarity. This distortion affords trigonal bipyramidal geometry at manganese, with the THF ligand in the trigonal plane. The resulting structure is depicted in Figure 1. Crystallographic information is provided in Table 1, and selected bond distances and angles are contained in Table 2. The Mn−O bond distance of 2.420(3) Å in **1** is long by comparison to the average value of 2.2 Å revealed by a search of Mn−O(THF) bond length in the Cambridge Structural Database.

Table 2. Selected Bond Distances and Angles[a]

compd	distances (Å)		angles (deg)	
1	Mn−N_{avg}	2.13(1)	N1−Mn−N2	75.7(1)
			N3−Mn−N1	162.1(1)
			N3−Mn−N2	113.0(1)
			N3−Mn−N4	75.7(1)
			N1−Mn−N4	111.3(1)
			N2−Mn−N4	130.3(1)
	Mn−O1	2.420(3)	N1−Mn−O1	79.9(1)
			N2−Mn−O1	114.7(1)
			N3−Mn−O1	82.3(1)
			N4−Mn−O1	115.0(1)
2	Mn−$N_{(TC)avg}$	2.00(3)	N1−Mn−N3	170.4(1)
	Mn−NO	1.699(3)	N2−Mn−N4	96.0(1)
	N−O	1.179(3)	N4−Mn−N5	134.5(1)
			N5−Mn−N2	129.5(1)
			Mn−N5−O1	174.1(3)
3	Mn−N_{avg}	1.98(4)	N1−Mn−N2*	99.46(8)
	Mn−O1B	2.09(4)	N2−Mn−N1*	177.5(1)
	Mn−O1A*	2.61(5)	N2−Mn−O1B	86.5(2)
	N3−O1B	1.26(15)	O1B−Mn−O1A*	51.3(7)
	N3−O1A*	1.2(2)	O1B−Mn−N1*	158.5(4)
			O1B−N3−O1A*	113(6)
			Mn−O1B−N3	110(8)
			Mn−O1A*−N3	89(6)

[a] Numbers in parentheses are estimated standard deviations of the last significant figure. Atoms are labeled as indicated in Figures 1−3.

Scheme 2

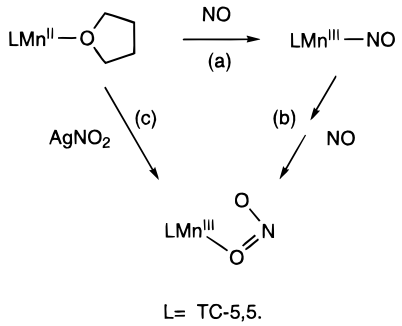

When treated with 1 equiv of NO, **1** converts cleanly to the mononuclear nitrosyl complex **2** (Scheme 2a). Exposure to NO results in an immediate and dramatic color change from green to dark red. The NO adduct forms irreversibly, with no loss of the nitrosyl occurring even after boiling a THF solution and applying a vacuum, or upon heating a solid sample to 100 °C under vacuum for 10 h. The structure of **2** exhibits several interesting features; an ORTEP diagram is provided in Figure 2 and bond distances and angles are summarized in Table 2. The average Mn−N distance for the TC nitrogen atoms has decreased from that in **1** to a value of 2.00(3) Å, consistent with a formal oxidation state change from Mn(II) to Mn(III), and in accord with that in related {Mn^{III}(TC-5,5)} complexes.[42] The Mn−NO distance of 1.699(3) Å and the N−O distance 1.179(3) Å are comparable to those found in MnNO porphyrin complexes.[18] The nearly linear, 174.1(3)°, Mn−N−O unit lies in the trigonal plane of **2**, rather than occupying the axial position of a square pyramid as occurs in the porphyrin analogues, which also contain linear Mn−N−O fragments.[18]

(36) Carlin, R. L. *Magnetochemistry*; Springer-Verlag: New York, 1986.
(37) Behere, D. V.; Mitra, S. *Inorg. Chem.* **1980**, *19*, 992−995.
(38) Mukherjee, A.; Spiro, T. G. *QCPE Bull.* **1995**, *15 (1)*, program 656.
(39) Wilson, E. B.; Decius, J. C.; Cross, P. C. *Molecular Vibrations*; McGraw- Hill: New York, 1955.
(40) Davis, W. M.; Zask, A.; Nakanishi, K.; Lippard, S. J. *Inorg. Chem.* **1985**, *24*, 3737−3743.
(41) Jaynes, B. S.; Doerrer, L. H.; Liu, S.; Lippard, S. J. *Inorg. Chem.* **1995**, *34*, 4, 5735−5744.
(42) Franz, K. J.; Lippard, S. J. Unpublished results.

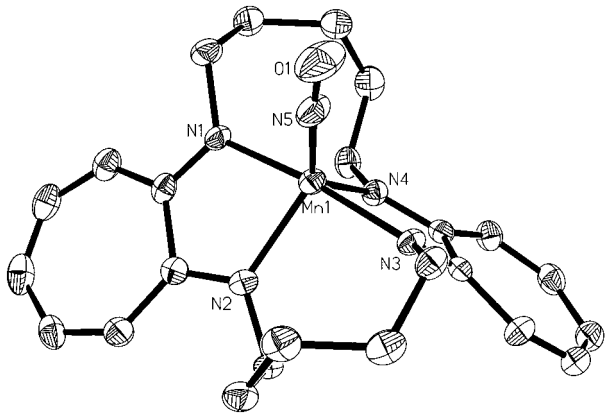

Figure 2. ORTEP diagram of [Mn(NO)(TC-5,5)] **(2)** showing selected atom labels and 50% probability ellipsoids for all non-hydrogen atoms.

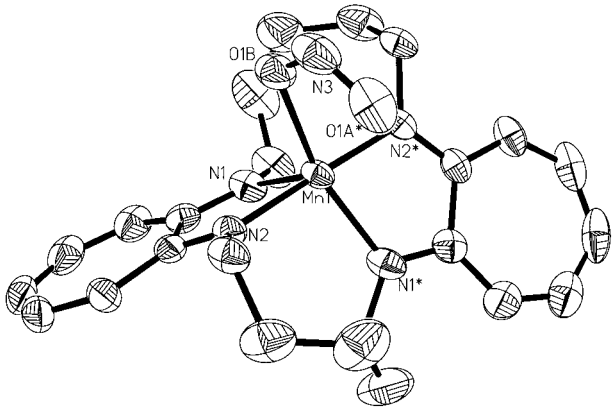

Figure 3. ORTEP diagram of [Mn(NO_2)(TC-5,5)] (**3**) showing selected atom labels and 50% probability ellipsoids for all non-hydrogen atoms. The asterisks refer to atoms generated by a 2-fold axis. Only one of two disordered nitrite ligands is shown; see text for details.

Compound **1** displays unusual reactivity when exposed to an excess amount of NO, forming the nitrito complex [Mn(NO_2)-(TC-5,5)], **3** (Scheme 2b). Only a few manganese nitrito complexes have been crystallographically characterized,[43−45] and **3** is unique in being obtained by reaction with NO. Exposure of the mononitrosyl complex **2** to either O_2 or NO also results in the formation of **3**, as evidenced by both UV−vis and IR spectroscopy. In addition, **3** can be independently synthesized by the oxidation of **1** with $AgNO_2$.

The average Mn−N distance in **3**, 1.98(4) Å, again signifies the Mn(III) oxidation state. The nitrito ligand is disordered over two positions, only one of which is depicted in the structure presented in Figure 3. The nitrito group coordinates in a monodentate fashion, with a Mn−O bond length of 2.09(4) Å. At a distance of 2.61(5) Å from manganese, the nonbonded oxygen atom assumes a cis orientation with respect to the metal atom.[46] There are two other structurally characterized mononuclear Mn nitrito complexes. One of these, [Mn(TPP)(NO_2)], has a trans monodentate O-bound coordination mode with a Mn−O bond length of 2.059(4) Å.[43] In the other, a seven-coordinate Mn^{II} complex containing the tetradentate, tripodal ligand tris(2-benzimidazolylmethyl)amine ligand, there is one trans monodentate O-bound nitrito group and one bidentate nitrito group having equivalent Mn−O distances of 2.32(9) Å.[44]

Electronic and Magnetic Properties. In the conventional notation[47] for metal nitrosyl complexes, **2** is designated as {MnNO}^{6} to avoid assigning formal oxidation states. There are intriguing differences, however, between **2** and other {MnNO}^{6} complexes; the NO stretching frequency is one of them. In THF solutions of **2**, this band appears at 1678 cm^{-1} (1676 cm^{-1} in CH_2Cl_2) and shifts to 1648 cm^{-1} upon isotopic labeling with ^{15}NO. This value agrees with the 1647.9 cm^{-1} value computed by assuming a classical diatomic oscillator model. In the solid state, the NO stretching mode appears at 1662 cm^{-1}, which is considerably lower in energy than the 1715−1735 cm^{-1} range reported for other manganese nitrosyls, including [Mn(NO)(ZSALDPT)],[17,48] and [Mn(NO)(TPP)].[18] These examples all have nearly linear Mn−N−O interbond angles and high NO stretching frequencies and were formally assigned as $Mn^{I}(NO^{+})$ species. The Mn−NO unit in **2** is also linear, but the X-ray structure and infrared data suggest that Mn is formally in a +3 oxidation state and that NO has been reduced. Although coordinated NO^{-} is often correlated with a bent Mn−N−O geometry, a molecular orbital analysis of the bonding in pentacoordinate metal nitrosyls predicts that an NO ligand in the equatorial plane of a trigonal bipyramid may assume a linear geometry even if formally assigned as NO^{-}.[49]

Further evidence for the formal assignment of **2** as a $\{Mn^{III}(NO^{-})\}^{2+}$ species comes from a normal-mode analysis of the Mn−N−O fragment. By using six experimental frequencies, the force constants were adjusted by least-squares refinement until the calculated and experimental values matched one another. The results indicate that, apart from the assignment of the high-frequency mode to the N−O stretch, the absorbance at 527 cm^{-1} derives from the Mn−N−O bend and the 504 cm^{-1} band from the Mn−N stretch. The force constant derived for the N−O stretch, 11.3 mdyn $Å^{-1}$, substantiates its NO^{-} character, the force constants of NO^{-}, NO, and NO^{+} being 8.4, 15.5, and 21.3 mdyn $Å^{-1}$, respectively.[50]

The magnetic susceptibilities of **2** and **3** were investigated by SQUID susceptometry, and plots of χ vs T and μ_{eff} vs T are presented in Figures 4 and S5 (see Supporting Information for Figure S5), respectively. Unlike diamagnetic compounds containing the formal $\{Mn^{I}(NO^{+})\}$ fragment,[17,18] **2** has an effective magnetic moment between 3.4 and 4.3 μ_B in the temperature range 5−300 K. The room-temperature effective moment of 4.3 μ_B is lower than the spin-only moment of 4.9 μ_B for an $S = 2$ system, but consistent with that of other high-spin Mn^{III} complexes in which $g < 2$.[37,51−53] The abrupt rise in μ_{eff} in the range $5 < T < 50$ K is characteristic of compounds with significant zero-field splitting (zfs).[36] The χ vs T data could be fit to the expression derived from the Hamiltonian $H = DS_z^2 + g\mu_B\mathbf{H}\cdot\mathbf{S}$,[37] where D is the zfs parameter and $S = 2$. The best fit was obtained for $D = \pm 5.6(4)$ cm^{-1} and $g = 1.6$. These values lie near the $1 < |D| < 4.9$ range found in related Mn(III) porphyrin[37,51,52] and Schiff-base complexes.[53] The nitrito compound **3** exhibits a negligible temperature dependence of

(43) Suslick, K. S.; Watson, R. A. *Inorg. Chem.* **1991**, *30*, 912−919.
(44) Lah, M. S.; Chun, H. *Inorg. Chem.* **1997**, *36*, 1782−1785.
(45) Kahn, O.; Bakalbassis, E.; Mathoniere, C.; Hagiwara, M.; Katsumata, K.; Ouahab, L. *Inorg. Chem.* **1997**, *36*, 1530−1531.
(46) Hitchman, M. A.; Rowbottom, G. L. *Coord. Chem. Rev.* **1982**, *42*, 55−132.
(47) Enemark, J. H.; Feltham, R. D. *Coord. Chem. Rev.* **1974**, *13*, 339−406.
(48) ZSALDPT = Schiff base pentadentate ligand of salicylaldehyde and 3,3′-bis(aminopropyl)amine.
(49) Hoffmann, R.; Chen, M. M. L.; Elian, M.; Rossi, A. R.; Mingos, D. M. P. *Inorg. Chem.* **1974**, *13*, 2666−2675.
(50) Brown, C. A.; Pavlosky, M. A.; Westre, T. E.; Zhang, Y.; Hedman, B.; Hodgson, K. O.; Solomon, E. I. *J. Am. Chem. Soc.* **1995**, *117*, 715−732.
(51) Dugad, L. B.; Behere, D. V.; Marathe, V. R.; Mitra, S. *Chem. Phys. Lett.* **1984**, *104*, 353−356.
(52) Yates, M. L.; Arif, A. M.; Manson, J. L.; Kalm, B. A.; Burkhart, B. M.; Miller, J. S. *Inorg. Chem.* **1998**, *37*, 840−841.
(53) Kennedy, B. J.; Murray, K. S. *Inorg. Chem.* **1985**, *24*, 1552−1557.

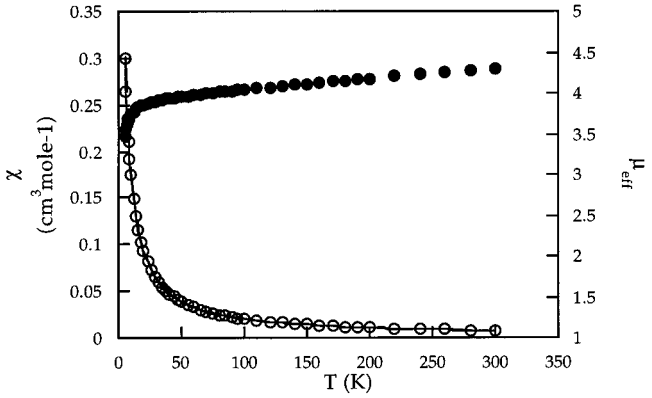

Figure 4. Average magnetic moment (μ_{eff}, ●); and magnetic susceptibility (χ, ○) for [Mn(NO)(TC-5,5)] (**2**). The magnetic susceptibility data were fit with $S = 2$ and the Hamiltonian described in the text, to give best fit parameters $D = \pm 5.2$ cm^{-1} and $g = 1.6$.

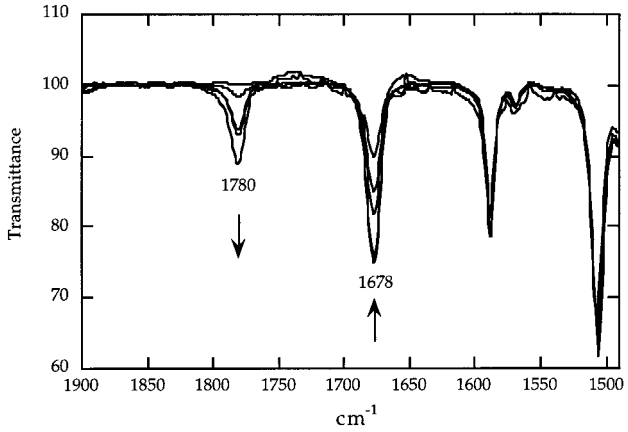

Figure 5. Overlay of the IR spectra resulting from the addition of NO to a THF solution of [Mn(NO)(TC-5,5)], **2**. The spectra were taken at −78 °C. The nitrosyl stretch at 1678 cm^{-1} decreases in intensity, while a new peak at 1780 cm^{-1} grows in. Excess NO over time results in complete disappearance of the 1678 cm^{-1} peak and a maximum for the peak at 1780 cm^{-1} (not shown here).

μ_{eff} from 50 to 300 K; the values range from 4.90 to 5.01 μ_B between these temperature limits, close to the spin-only moment for $S = 2$. The effect of zfs is manifest below 50 K, and a fit of χ vs T, as described above, revealed a large D value of ±7.5(5) cm^{-1} and $g = 2.0$. Both compounds **2** and **3** are EPR silent at room temperature and at 77 K,[42] and it was therefore not possible to obtain a direct measure of g.

Reactivity Studies. The nitrosyl bands in the IR spectrum provide a convenient means by which to follow the reaction of **1** with NO. A clear assignment of bands arising from coordinated NO_2^- was prevented by strong ligand absorptions in the anticipated regions of the spectrum.[46] Figure 5 displays the spectral changes which result from the addition of an increasing number of equivalents of NO to a THF solution of **1**. The first equivalent (based on Mn^{II}) of NO results in the formation of mononitrosyl species **2**, with ν_{NO} at 1678 cm^{-1}. A new absorbance appears at 1780 cm^{-1} when an additional 0.5 equiv of NO is added, and this feature continues to increase in intensity at the expense of the 1678 cm^{-1} band. After approximately 2 equiv of NO were added, a third peak (not shown) appears at 2223 cm^{-1} that corresponds to gaseous N_2O. When the solution is purged with N_2 or evacuated, the peak at 1780 cm^{-1} disappears to reveal a spectrum matching that of **3**. This result suggests that the absorbance at 1780 cm^{-1} arises from a weak interaction between the nitrito product **3** and NO.

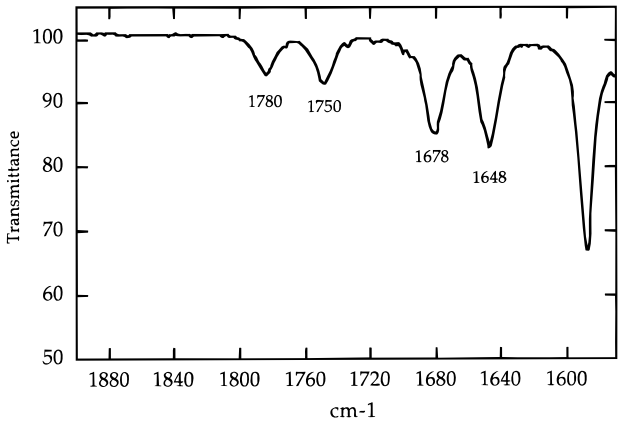

Figure 6. IR spectrum taken at room temperature after addition of 1.2 equiv of ^{15}NO to a THF solution of [Mn(^{14}NO)(TC-5,5)] (**2**). The ^{14}NO stretch appears at 1678 cm^{-1}, and the ^{15}NO stretch appears at 1648 cm^{-1}. The new peak that appears at 1780 cm^{-1} also has a ^{15}NO-sensitive peak at 1750 cm^{-1}.

In support of this assignment, exposure of an authentic sample of **3** to NO similarly led to the reversible formation of a band at 1780 cm^{-1}. In addition, a preliminary crystal structure that is consistent with a [Mn(NO)(NO_2)(TC-5,5)] formulation was obtained from a crystal grown by slowly diffusing pentane into a benzene solution of **3** under an NO atmosphere.[42]

The appearance of N_2O and of the 1780 cm^{-1} band assigned to the nitrito/nitrosyl species after the addition of only slightly more than 1 equiv of NO to **1** indicates fast reaction kinetics, where any intermediate reacts rapidly with NO to afford **3**. This observation is similar to those made in kinetic studies of the CuNO system.[10] Preliminary UV−vis experiments revealed isosbestic points in the spectra of solutions of **2** when NO was incrementally introduced, suggesting a clean and rapid transformation of reactant to product, with no build up of any intermediates.[42]

Although such rapid reactivity has thus far not allowed us to detect an intermediate spectroscopically, it is likely that a transient dinitrosyl $Mn(NO)_2$ or hyponitrito $Mn(N_2O_2)$ species forms. Both have been previously postulated in mechanistic consideration of NO reduction to N_2O, but neither has been definitively detected.[7,10,54,55] Mixed-labeling experiments shown in Figure 6 provide indirect evidence for a dinitrosyl intermediate in our system. When [Mn(^{14}NO)(TC-5,5)] was exposed to 1.2 equiv of ^{15}NO in THF solution, the mononitrosyl stretch at 1678 cm^{-1} split into two peaks of equal intensity, one at 1678 and one at 1648 cm^{-1}. An absorbance at 1780 cm^{-1}, attributed to a nitrito/nitrosyl species as suggested above, also appeared together with its ^{15}NO counterpart at 1750 cm^{-1}. The binding of NO to **1** is irreversible, both in solution and in the solid state, so the appearance of a statistical mixture of bands arising from {Mn^{15}NO} and {Mn^{14}NO} fragments could be the result of a dinitrosyl intermediate in an associative mechanism for ^{14}NO/^{15}NO exchange. An equilibration such as that shown in Scheme 3 would explain the complete scrambling of labels in the

Scheme 3

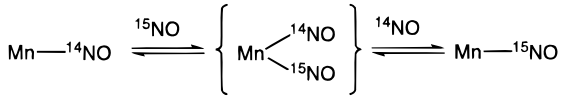

(54) MacNeil, J. H.; Berseth, P. A.; Bruner, E. L.; Perkins, T. L.; Wadia, Y.; Westwood, G.; Trogler, W. C. *J. Am. Chem. Soc.* **1997**, *119*, 1668−1675.

(55) Yoshimura, T. *Inorg. Chim. Acta* **1984**, *83*, 17−21.

Table 3. Results of Headspace Analysis of N_2O and NO after Reaction of **1** with NO[a]

	starting material **1**, μmol	starting material NO, μmol	equiv of NO per **1**	N_2O generated (μmol)	equiv of N_2O per **1**	NO in headspace (μmol)	equiv of per **1**	NO consumed (μmol)	equiv of NO consumed per **1**
a[b]	29	146	5	28(3)	1	38(3)	1.3	108(3)	3.6−3.8
b[b]	28	168	6	27(2)	1	44(4)	1.6	124(4)	4.2−4.6
c[c]	28	084	3	22(2)	0.79	14(1)	0.5	70(1)	2.5

[a] See text for details. [b] Sampled after 48 h. [c] Sampled after 24 h.

formation of N_2O, as confirmed by the appearance (Figure S4) of IR peaks at 2223 ($\nu^{14}N_2O$), 2200 ($\nu^{14}N^{15}NO$), 2177 ($\nu^{15}N^{14}NO$), and 2153 cm^{-1} ($\nu^{15}N_2O$).

Mechanism. The overall reaction sequence for the disproportionation of NO is summarized in eqs 2−4. Analysis of NO and N_2O gases in the headspace by GC provides support

$$[Mn(THF)(TC\text{-}5,5)] + NO \rightarrow [Mn(NO)(TC\text{-}5,5)] \quad (2)$$

$$[Mn(NO)(TC\text{-}5,5)] + xNO \rightarrow \{Mn(NO_2)(NO)(TC\text{-}5,5)\} + N_2O + (x-4)NO \quad (3)$$

$$\{Mn(NO_2)(NO)(TC\text{-}5,5)\} \rightleftharpoons [Mn(NO_2)(TC\text{-}5,5)] + NO \quad (4)$$

for the stoichiometry as written. Table 3 shows the results of three different experiments, where varying amounts of NO were allowed to react with **1**. Experiments *a* and *b* were both analyzed after 48 h of reaction time, and both reveal that ∼4 equiv of NO were consumed per Mn atom. Experiment *c*, in which only 3 equiv of NO was initially present, was sampled after 24 h of reaction time. The amount of NO still remaining in the headspace indicated that only 2.5 equiv of NO had been consumed, which is more likely to be the result of insufficient NO to provide a driving force than a shorter reaction time.

In Scheme 4 we propose a mechanism for the disproportionation of NO. The first step (a) involves the oxidation of Mn^{II} by 1 equiv of NO to form the well-characterized $\{MnNO\}^6$ compound **2**, which in a formal sense behaves as $\{Mn^{III}NO^-\}^{2+}$. Addition of another equivalent of NO could afford either a dinitrosyl or a hyponitrito intermediate. Given the results of the mixed labeling experiments, we favor initial formation of a dinitrosyl, as indicated in path b, which could directly convert to a hyponitrito species, as suggested in (c). Alternatively, another equivalent of NO could induce N−N coupling of the dinitrosyl species, as presented in (d). This pathway is analogous to the CO-induced coupling of dinitrosyls proposed by others.[56,57] Addition of one or two more equivalents of NO could then result in attack of NO on the hyponitrito intermediate, coordination of the oxygen of the nitrito ligand, simultaneous loss of N_2O, and weak binding of NO, affording the nitrito/nitrosyl species (e). The identity of such an intermediate has been verified crystallographically.[42] Evacuation removes the weakly coordinated nitrosyl to give the final Mn nitrito product **3**, step f. The headspace analysis supports the overall stoichiometry, and IR evidence confirms the reversible interconversion of the nitrito and the nitrito-nitrosyl species.

Scheme 4

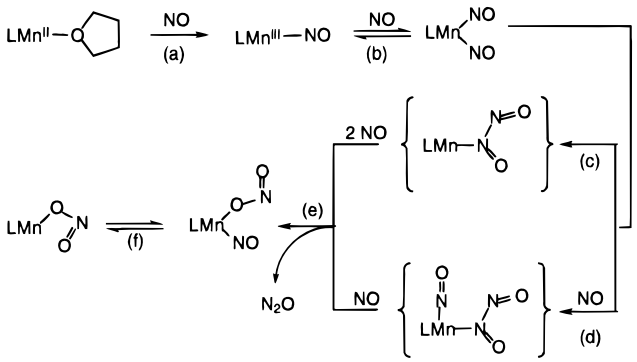

Summary and Conclusions

The tropocoronand ligand TC-5,5 provides a framework for trigonal-bipyramidal 5-coordinate metal nitrosyls, where NO is forced to lie in the equatorial plane. Steric constraints make alternative square-pyramidal geometry highly unlikely.[58] In addition, the strongly electron-releasing nature of the tropocoronand ligand system favors reduction of the bound nitrosyl, resulting in formation of a linear, formally $\{Mn^{III}NO^-\}^{2+}$ fragment. As a consequence of these effects, manifest in [Mn(NO)(TC-5,5)], addition of excess NO results in the formation of N_2O and metal-bound NO_2. The present investigation strongly supports previous arguments that a coordinated NO^- ligand is required to activate reductively NO to form N_2O.[59] Previous metal-induced NO disproportionation reactions involved later transition metals.[5,6] This first example of Mn-induced NO activation extends the scope and generality of metal-NO chemistry in a manner that has significant consequences for both the biological and environmental reactivity of nitric oxide.

Acknowledgment. This work was supported by grants from the National Science Foundation. We thank Dr. Peter Fuhrmann for help with X-ray crystallography and D. P. Steinhuebel and Dr. J. Du Bois for many helpful discussions.

Supporting Information Available: Figures S1−S3, displaying fully labeled ORTEP diagrams for each reported structure, Figure S4, displaying an IR spectra of the formation of mixed-labeled N_2O, and Figure S5, displaying the plots of χ vs T and μ_{eff} vs T for **3** (6 pages, print/PDF). X-ray crystallographic files, in CIF format, are available on the Internet only. See any current masthead page for ordering information and Web access instructions.

JA981410E

(56) Bhaduri, S.; Johnson, B. F. G.; Savory, C. J.; Segal, J. A.; Walter, R. H. *J. Chem. Soc., Chem. Commun.* **1974**, 809−810.
(57) Haymore, B. L.; Ibers, J. A. *J. Am. Chem. Soc.* **1974**, *96*, 3325−3327.
(58) Jaynes, B. S.; Ren, T.; Liu, S.; Lippard, S. J. *J. Am. Chem. Soc.* **1992**, *114*, 9670−9671.
(59) McCleverty, J. A. *Chem. Rev.* **1979**, *79*, 53−76.